

# Impurity state in the vortex core of $d$ -wave superconductors: Anderson impurity model versus unitary impurity model

Qiang Han,<sup>1,2</sup> Z. D. Wang,<sup>1,2,3\*</sup> X. -G. Li,<sup>1</sup> and Li-yuan Zhang<sup>4</sup>

<sup>1</sup>*Structure Research Laboratory, Department of Material Science and Engineering, University of Science and Technology of China, Hefei Anhui 230026, China*

<sup>2</sup>*Department of Physics, University of Hong Kong, Pokfulam Road, Hong Kong, China*

<sup>3</sup>*Texas Center for Superconductivity, University of Houston, Texas 77204, USA*

<sup>4</sup>*Department of Physics, Peking University, Beijing 100871, China*

Using an extended Anderson/Kondo impurity model to describe the magnetic moments around an impurity doped in high- $T_c$   $d$ -wave cuprates and in the framework of the slave-boson meanfield approach, we study numerically the impurity state in the vortex core by exact diagonalization of the well-established Bogoliubov-de Gennes equations. The low-energy impurity state is found to be in good agreement with scanning tunneling microscopy observation. After pinning a vortex on the impurity site, we compare the unitary impurity model with the extended Anderson impurity model by examining the effect of the magnetic field on the impurity state. We find that the impurity resonance in the unitary impurity model is strongly suppressed by the vortex; while it is insensitive to the field in the extended Anderson impurity model.

PACS numbers: 74.25.Jb, 72.15.Qm, 74.60.Ec, 73.20Hb

Effects of nonmagnetic impurities, such as Zinc, doped in the  $\text{CuO}_2$  plane of high- $T_c$  materials have attracted much attention in recent years as it may help us to better understand the underlying mechanism of high- $T_c$  superconductivity<sup>1</sup>. The low-energy (near zero) impurity resonant state in  $d$ -wave superconductors was first predicted in Refs.<sup>2–4</sup> based on a unitary scattering-potential impurity model and later successfully observed in a series of beautiful atomic-scale scanning tunneling microscopy (STM) experiments<sup>5–7</sup> in the vicinity of individual Zn ions in  $\text{Bi}_2\text{Sr}_2\text{Ca}(\text{Cu}_{1-x}\text{Zn}_x)_2\text{O}_{8+\delta}$ . Since  $\text{Zn}^{++}$  has no spin itself (therefore nonmagnetic), it is natural to treat the impurity as a point-like scalar potential scatterer of conduction electrons. Indeed, both energy position and four-fold symmetric spatial distribution<sup>7</sup> of local density of states (LDOS) of quasiparticle can be explained consistently by theoretical calculations based on the  $t$ -matrix scattering potential theory in the unitary limit<sup>3</sup>. Nevertheless, the sign and magnitude of the scattering potential as well as the particle-hole symmetry play a crucial role in determining the exact energy level of impurity resonant state relative to Fermi energy. The scattering potential chosen in various theoretical studies differ largely from  $-4.4$  eV to  $18.9$  eV<sup>8–10</sup>. The continuum  $t$ -matrix theory, which assumed particle-hole symmetry and *repulsive* potential, predicted impurity state with energy<sup>3</sup> consistent with STM observation<sup>7</sup> that the resonance lies slightly below the Fermi level; on the other hand, the particle-hole symmetry is not applicable to high- $T_c$  cuprates and theoretical calculations<sup>9,10</sup> show that in the absence of such symmetry only strong *attractive* potential can produce impurity state with negative energy while repulsive potential<sup>10</sup> gives positive energy contrary to experiment results. Furthermore, the unitary impurity model has difficulty in accounting for spectra distribution pattern of differential conductance at the resonance energy. The experiment shows that the zero bias peak is strongest on the Zn ion with local maximum on its second nearest neighbor Cu sites<sup>7</sup> while the unitary impurity model concluded that the spectral weight on Zn atom is negligibly small and local maximum peaks are on nearest neighbor Cu sites of the impurity<sup>3,11,10</sup>. In order to reconcile the apparent discrepancy, the effect of the interlayer tunneling matrix elements, such as a blocking effect of BiO layer<sup>11</sup> and a fork model<sup>10</sup> have been employed to reproduce the distribution of spectral weight. At present, whether the spatial pattern of the tunneling conductance of the impurity resonance is intrinsic in the  $\text{CuO}_2$  plane or interlayer tunneling effect must be considered is still an open question for both theoretical investigation and further experimental examination. Recently, several alternative theoretical models<sup>8,9,12,13</sup> have been suggested, which take the effect of the Kondo screening of the local magnetic moments induced around the Zinc atom into account, mostly motivated by the observation of nuclear magnetic resonance (NMR)<sup>14–16</sup> and neutron scattering experiments<sup>17,18</sup> that staggered magnetic moments are developed around Zn ion with total net spin  $1/2$ . When Kondo spin dynamics of such moment is considered, by including an exchange interaction between the induced spin and the spin of conduction electrons in the model Hamiltonian, Polkovnikov *et al*<sup>9</sup> produce an impurity state whose energy dependence and spatial pattern may fit well with STM spectra, without a strong scattering potential and the specific characteristic of interlayer tunneling matrix elements.

Motivated by the above controversy between the unitary impurity model and the model invoking induced magnetic moments, in this work we intend to compare these two models in the case that a single vortex line is pinned by the

---

\*To whom correspondence should be addressed. Email address: zwang@hkucc.hku.hk

impurity. To describe the Kondo effect of the magnetic moments and the effect of vortex, we introduce an extended Anderson impurity model with a phase factor being dependent on site and vortex. In the absence of vortex, both models with appropriate parameters can generate low-lying impurity state. However, when a vortex is present, for the unitary impurity model, the pronounced LDOS peak generated around the Zn impurity is largely decreased or even destroyed, indicating the vanishing of the impurity resonance by the vortex core; while for the extended Anderson impurity model, the existence of the vortex center has a weak effect on the impurity state. Such a difference may be examined readily by STM experiments on  $\text{Bi}_2\text{Sr}_2\text{Ca}(\text{Cu}_{1-x}\text{Zn}_x)_2\text{O}_{8+\delta}$  samples subject to a strong magnetic field.

In this work, we adopt an extended Hubbard model on a two dimensional (2D) lattice with nearest-neighbor (NN) hopping and NN pairing interaction to model the  $d$ -wave high- $T_c$  cuprates and the extended Anderson impurity model to describe the magnetic moments around the impurity(Zinc ion) doped in the  $\text{CuO}_2$  plane. The model Hamiltonian is expressed as

$$H = H_{\text{dsc}} + H_{\text{imp}} \quad (1)$$

where

$$H_{\text{dsc}} = - \sum_{\langle i,j \rangle \sigma} t_{ij} c_{i\sigma}^\dagger c_{j\sigma} + \sum_{\langle i,j \rangle \sigma} (\Delta_{ij} c_{i\uparrow}^\dagger c_{j\downarrow}^\dagger + \text{h.c.}) - \sum_{i,\sigma} \mu c_{i\sigma}^\dagger c_{i\sigma}, \quad (2)$$

and

$$H_{\text{imp}} = H_{\text{mag}} + V_I c_{0\sigma}^\dagger c_{0\sigma}. \quad (3)$$

Here  $H_{\text{dsc}}$  is the BCS-like Hamiltonian of the host  $d$ -wave superconductor described on a 2D lattice.  $\langle i,j \rangle$  refers to the NN sites and  $t_{ij}$  the hopping integral between site  $i$  and  $j$ .  $\mu$  is the chemical potential.  $\Delta_{ij}$  is the bond paring potential defined as  $\Delta_{ij} = -V_d \langle c_{i\downarrow} c_{j\uparrow} \rangle$  with  $V_d$  the effective pairing strength between electrons on NN sites.  $H_{\text{imp}}$  represents the impurity Hamiltonian which includes both an on-site scattering potential term represented by  $V_I$  and the term  $H_{\text{mag}}$  describing the local moments around the impurity. As suggested by NMR experiments<sup>14–16</sup>, the induced magnetic moments with net spin 1/2 are mainly located at the four NN Cu sites of the central Zn impurity site  $\mathbf{r}_0 = (0, 0)$  while negligible right on the Zn site; therefore as in Ref.<sup>9</sup>, we assume that the magnetic impurity with an effective 1/2 spin may reside only in the NN sites and couples with conduction electrons on the NN sites. Namely, the  $H_{\text{mag}}$  may be modeled by the extended Anderson impurity model with strong Hubbard repulsion  $U_d$  as  $H_{\text{mag}} = \sum_{\sigma} \epsilon_d d_{\sigma}^\dagger d_{\sigma} + U_d d_{\uparrow}^\dagger d_{\uparrow} d_{\downarrow}^\dagger d_{\downarrow} + \sum_{\mathbf{r}_i=\boldsymbol{\tau},\sigma} V_h(i) (e^{\phi_i} c_{i\sigma}^\dagger d_{\sigma} + \text{h.c.})$  with  $\boldsymbol{\tau} = \pm \hat{\mathbf{x}}, \pm \hat{\mathbf{y}}$  unit vectors, where  $\epsilon_d$  is the d-electron energy level and  $V_h$  is the hybridization of the moments with the conduction electrons. As a modification to the coupling term in the ordinary Anderson impurity model, we here introduce a site-dependent phase factor  $\phi_i$ , which is found to be quite crucial in determining the energy level and even the existence of the impurity state if  $V_I$  is not so strong. Note that under the meanfield decoupling scheme of Ref.<sup>19</sup>, the present model for  $H_{\text{mag}}$  is essentially equivalent to the magnetic impurity(Kondo) model in Ref.<sup>9</sup>, where it is written as  $\sum_i K_i \mathbf{S} \cdot \mathbf{s}(i)$  with the summation being over the NN sites of the impurity, and  $\mathbf{S} = \sum_{\alpha\beta} d_{\alpha}^\dagger \sigma_{\alpha\beta} d_{\beta} / 2$  and  $\mathbf{s} = \sum_{\alpha\beta} c_{\alpha}^\dagger \sigma_{\alpha\beta} c_{\beta} / 2$  representing respectively the spin operators of the magnetic impurity and the conduction electrons. This is because that this spin-exchange term can be transformed by the mean-field decoupling scheme in Ref.<sup>19</sup>:  $K \sum_i \mathbf{S} \cdot \mathbf{s}(i) \rightarrow -3K/8 \sum_{\sigma} [\chi_i^* c_{i\sigma}^\dagger d_{\sigma} + \text{h.c.}]$ , where a *complex* Hubbard-Stratonovich field  $\chi_i = \langle c_{i\sigma}^\dagger d_{\sigma} \rangle$  is introduced as an effective hopping amplitude between the d-level and conduction electrons. At this stage, one can see clearly that the phase factor  $\phi_i$  introduced in our model and that of the field  $\chi_i$  are closely related. Assuming the four-fold rotational symmetry with respect to the impurity site, there are four inequivalent arrangements of  $\phi_{\boldsymbol{\tau}}$ , that is

$$\phi_{\boldsymbol{\tau}}^{(m)} = m \times \theta(\boldsymbol{\tau}), \quad (4)$$

with  $m = 0, 1, 2, 3$ ,  $\theta(\pm \hat{\mathbf{x}}) = (\pi/2) \mp (\pi/2)$ , and  $\theta(\pm \hat{\mathbf{y}}) = \pm (\pi/2)$ . In Ref.<sup>9</sup>, a nontrivial  $d$ -wave pattern of  $\chi_i$  has been found to have the lowest free energy saddle point, whose phase corresponds to  $m = 2$ , matching the underlying symmetry of local bond pairing potential  $\Delta_{0,i}$ . When the vortex exists, the symmetry of the underlying pairing potential would change from the local  $d$ -wave pattern to that responding to the winding of phase. Therefore, it appears reasonable to expect that  $\phi$  might change from  $m = 2$  to  $m = 1$  as a vortex is pinned at the impurity site. We find that such a response of  $\phi$  to the magnetic field is quite crucial in keeping the impurity state in the vortex core.

In the treatment of the extended Anderson impurity model at low temperatures,  $U_d$  is assumed to be infinite as usual, which forbids double occupancy of electrons on the d-level. Therefore, the slave-boson mean-field theory<sup>20,21</sup> can be applied as in Refs.<sup>8,22</sup> where the d-electron operator is written as  $d_{\sigma}^\dagger = f_{\sigma}^\dagger b$  with  $f_{\sigma}$  the spin-carrying fermion operator and  $b$  the holon operator. Furthermore, the single occupancy constraint  $\sum_{\sigma} f_{\sigma}^\dagger f_{\sigma} + b^\dagger b = 1$  should be obeyed.

At the mean-field level, the holon operators  $b$  and  $b^\dagger$  are approximated by a  $c$ -number  $b_0$  and the constraint is enforced on average by introducing a Lagrange multiplier  $\lambda_0$ . Accordingly, the mean-field  $H_{\text{imp}}$  becomes

$$H_{\text{imp}} = \sum_{\sigma} \tilde{\epsilon}_d f_{\sigma}^{\dagger} f_{\sigma} + \sum_{\mathbf{r}_i=\boldsymbol{\tau},\sigma} \widetilde{V}_h(i) (e^{i\phi_i} c_{i\sigma}^{\dagger} f_{\sigma} + \text{h.c.}) + V_I c_{0\sigma}^{\dagger} c_{0\sigma} + \lambda_0 (b_0^2 - 1) \quad (5)$$

with renormalized parameters  $\tilde{\epsilon}_d = \epsilon_d + \lambda_0$  and  $\widetilde{V}_h = V_h b_0$ . By applying the self-consistent mean-field approximation and performing the Bogoliubov transformation, diagonalization of the Hamiltonian can be achieved by solving the following Bogoliubov-de Gennes(BdG) equations:

$$\sum_j \begin{pmatrix} H_{i,j} & \Delta_{i,j} \\ \Delta_{i,j}^* & -H_{i,j}^* \end{pmatrix} \begin{pmatrix} u_j^n \\ v_j^n \end{pmatrix} = E_n \begin{pmatrix} u_j^n \\ v_j^n \end{pmatrix} \quad (6)$$

where  $u^n, v^n$  are the Bogoliubov quasiparticle amplitudes with corresponding eigenvalue  $E_n$  and  $H_{i,j} = -\delta(\mathbf{r}_i + \boldsymbol{\tau} - \mathbf{r}_j)[t_{i,j \neq i_d} - (\delta_{i,i_d} + \delta_{j,i_d})\widetilde{V}_h e^{i\phi_{\tau}}] - \delta_{i \neq i_d, j}[\mu - \delta(\mathbf{r}_i - \mathbf{r}_0)V_I] + \delta_{i,i_d}\tilde{\epsilon}_d$ . Here,  $i, j$  represent the index of the 2D lattice sites with  $i_d$  as the index for the magnetic moment residing on the NN sites of the doped impurity.  $\Delta_{i,j}$  is defined between a pair of NN sites on the 2D lattice and is calculated according to the self-consistent condition:

$$\Delta_{i,j} = \frac{V_d}{2} \sum_n (u_i^n v_j^{n*} + u_j^n v_i^{n*}) \tanh\left(\frac{E_n}{2k_B T}\right) \quad (7)$$

and

$$b_0^2 = 1 - 2 \sum_n \{|u_{i_d}^n|^2 f(E_n) + |v_{i_d}^n|^2 [1 - f(E_n)]\} \quad (8)$$

Once the BdG Eq. 6 is solved self-consistently, the quasiparticle spectrum can be obtained and the LDOS proportional to the differential tunneling conductance observed in STM experiments is given by

$$\rho(\mathbf{r}_i, E) = - \sum_n [|u_i^n|^2 f'(E_n - E) + |v_i^n|^2 f'(E_n + E)] \quad (9)$$

where  $f(E)$  represents the Fermi distribution function.

*Unitary Impurity Model.*— First, we study the variation of the impurity state when a vortex line is sitting on the impurity site within a unitary impurity model. Exact diagonalization is applied and the BdG equations are solved self-consistently. In studying the electronic structure of vortex lattice in  $d$ -wave superconductors, a magnetic unit cell which accommodates two vortices is usually employed in numerical studies<sup>23–27</sup>. Such a method has been applied to treat impurity effect in the mixed state of  $s$ -wave<sup>28</sup> and  $d$ -wave<sup>29</sup> superconductors. The primitive translation vectors of the magnetic unit cell are  $\mathbf{R}_x = aN_x \hat{x}$  and  $\mathbf{R}_y = aN_y \hat{y}$ , where  $a$  is the lattice constant and will be set as unity. The pairing potential winds by  $4\pi$  around the magnetic unit cell. The quasiparticle amplitudes  $u^n$  and  $v^n$  are classified by the magnetic Bloch quasi-momentum  $\mathbf{k}$ .

The parameters we choose are  $\mu = -0.2t$ ,  $V_d = 2.2t$  which give rise to  $\Delta_d = 0.274t$  (accordingly  $\Delta_{\text{max}} \simeq t$ ) and  $T_c = 0.45t$ . We here intentionally take a relatively large amplitude of the energy gap  $\Delta_{\text{max}}$  with respect to real materials, because a large energy gap can sufficiently lower the LDOS peak corresponding to the vortex core states and in our case a broad structure is achieved near the vortex center<sup>30</sup>, which enables us to distinguish the LDOS peak of the unitary impurity from that corresponding to the vortex core states. The on-site attractive scattering potential is chosen as  $V_I = -10t$ . In Fig. 1 the LDOS at the NN site of Zn site is plotted. In the absence of magnetic field(dashed line), a sharp peak is found at  $E_0/\Delta_{\text{max}} = -0.02$  corresponding to the impurity resonance. In the inset, the spatial distribution of the LDOS at resonance energy,  $\rho(\mathbf{r}, E_0)$  is shown, indicating that the spectral weight is concentrated at the NN sites of the impurity while vanishingly small at the impurity site. These results are qualitatively consistent with previous numerical investigations. When a vortex is pinned right on the impurity site, from Fig. 1(solid line) we can see that the LDOS peak at the NN site of Zn is significantly suppressed and mixes with the vortex core states without identification of impurity resonance state any more. As a strong scattering potential, the unitary impurity can drive the spectral weight on it mainly to its NN sites no matter vortex is present or not. However, in the absence of vortex, the LDOS at a specific energy is raised, leading to a resonance state; while in the presence of vortex, the LDOS on NN sites is increased in a wide energy range as seen in Fig. 1 and thus it is more reasonable to state that the vortex core states are strengthened by the impurity scattering. Broadening of the impurity resonance state by the magnetic field exists when the supercurrent of the vortex disturbs the energy spectrum of  $d$ -wave superconductors *via*

Doppler shift<sup>31</sup>. However, in our case the smearing of the impurity resonance state is not induced by the supercurrent because the impurity is on the vortex center where supercurrent is zero. We attribute it to the nature of topological singularity of the vortex center where the phase of pairing potential varies arbitrarily, which makes the vortex center itself a strong scatter of electrons<sup>32</sup>. Therefore, it is the vortex that modifies the background electronic structure which is responsible for the impurity resonance and accordingly makes the impurity resonance indiscernible.

*Extended Anderson Impurity Model.*— We now address the impurity state in the presence of Kondo screening of the magnetic moments described by the extended Anderson impurity model. First we consider the case in the absence of applied magnetic field. We set  $m = 2$  in Eq. (4) in consideration of free energy minimization<sup>9</sup>. The exact diagonalization is performed on a  $24 \times 24$  square lattice, which is seen to be sufficiently large due to the localized feature of the impurity state. The scattering potential  $V_I$  is simplified as zero (The role of nonzero  $V_I$  will be discussed later). The bare d-level is set as  $\epsilon_d = -4t$  and the coupling strength  $V_h = 2t$  (Kondo screening regime). The value of the Lagrange multiplier  $\lambda_0$  is determined by minimizing the free energy of the system as indicated in the inset of Fig. 2 and the corresponding value of  $b_0$  is calculated self-consistently according to Eq. (8). In the inset of Fig. 2,  $\Delta F$  as a function of  $\lambda_0$  is plotted, where  $\Delta F$  represents the change of the free energy when the local magnetic moments couple with conduction electrons. We find that for the chosen parameters the lowest free energy occurs when  $\lambda_0 \simeq 5.6t$  with  $b_0 \simeq 0.64$ . Figure 2 gives LDOS's on the Zn site, its NN site and NNN site. There is a sharp peak at the energy  $E_0/\Delta_{max} = -0.04$ , which is well consistent with STM measurement. Right on the Zn site, the peak is strongest and local maximum peaks are on the NNN sites; while on the NN sites peaks are rather weak and at  $-E_0/\Delta_{max} = 0.04$ . The spatial distribution of LDOS at  $E_0$  is shown in the inset of Fig. 2, also in agreement with STM spectra<sup>7</sup> and a theoretical study based on another approach on an essentially equivalent model<sup>9</sup>. Our analysis shows that the impurity state induced by the magnetic moment is a bound state with a very short attenuation length  $\sim \sqrt{2}a$ .

Recent STM measurements<sup>33</sup> of impurity states induced by Zn<sup>++</sup> and Mg<sup>++</sup> doped in YBa<sub>2</sub>CuO<sub>6.9</sub> reported that the resonance energies are at  $(-10 \pm 2)$  and  $(4 \pm 2)$  meV, being not necessarily near zero bias. Based on our model, with the fixed coupling strength e.g.  $V_h = 2t$ , both the bare d-level  $\epsilon_d$  and on-site scattering potential  $V_I$  could adjust the resonance position of the impurity state. When  $V_I = 0$  and  $\epsilon_d$  ranges from 0 to  $-4t$ ,  $E_0/\Delta_{max}$  varies from  $-0.18$  to  $-0.04$ . An attractive(negative)  $V_I$  drives the energy position below the Fermi level further (e.g. when  $V_I = -1t$ ,  $E_0/\Delta_{max}$  varies from  $-0.42$  to  $-0.26$  as  $\epsilon_d$  ranges from 0 to  $-4t$ ), while repulsive one makes the resonance energy approach to or even across the Fermi level and become positive (e.g. when  $V_I = t$ ,  $E_0/\Delta_{max} = 0.25$  with  $\epsilon_d = -4t$ ). However, too large  $V_I$  ( $\gg t$ ) can affect the spin-induced impurity state strongly and double resonance peaks<sup>13</sup> are found in the unitary limit, which disagrees with the STM spectra.

When a vortex is pinned on the impurity site, we expect that there is a rearrangement of  $\phi_{\mathcal{T}}^{(m)}$  according to the winding of the phase of the order parameter so that the phases of the Hubbard-Stratonovich field  $\chi_i$  and the local bond pairing potential between NN sites  $\Delta_{0,i}$  have the best match. Therefore,  $m$  will vary from 2 to 1 when a vortex is present. This is quite important as other choices of  $m$  (0, 2, 3) are found to result in the disappearing of the impurity state. The numerical results are shown in Fig. 3, which plots the LDOS as a function of energy on the impurity site. A strong single peak is seen near the Fermi level, indicating that the impurity state still survives under the field. Being different from the case without vortex, the peak is lowered slightly and moved to positive bias  $E_0/\Delta_{max} = 0.02$ , while the spatial pattern of the impurity state is not modified (see the inset of Fig. 3).

In summary, we have compared the extended Anderson impurity model with the unitary impurity model by studying numerically the impurity state of a  $d$ -wave superconductor as a vortex is pinned on the impurity site. We find that the impurity resonance governed by the scattering potential mechanism is sensitive to the presence of vortex, while the impurity bound state generated from the magnetic moments mechanism seems rather robust to the field. Therefore, it may be helpful to clarify the dominant mechanism of the impurity state in Zn or Mg impurities doped cupates by examining the existence of the impurity resonance, the variation of its energy, and even the STM spatial pattern in the presence of a strong magnetic field.

We thank Profs. C. S. Ting, J. L. Zhang, and Dr. Y. Chen for helpful discussions. The work was supported by a RGC grant of Hong Kong under Grant No. HKU7144/99P and the 973-project of the Ministry of Science and Technology of China under Grant Nos. G1999064602&G1999064603. ZDW acknowledges partial support from the Texas Center for Superconductivity at the University of Houston.

---

<sup>1</sup> A. V. Balatsky, Nature **403**, 717 (2000).

- <sup>2</sup> A. V. Balatsky, M. I. Salkola, and A. Rosengren, Phys. Rev. B **51**, 15547 (1995).
- <sup>3</sup> M. I. Salkola, A. V. Balatsky, and D. J. Scalapino, Phys. Rev. Lett. **77**, 1841 (1996).
- <sup>4</sup> M. E. Flatte, J. M. Byers, Phys. Rev. B **56**, 11213 (1997).
- <sup>5</sup> E. W. Hudson, S. H. Pan, A. K. Gupta, K. -W. Ong, and J. C. Davis, Science **285**, 88 (1999).
- <sup>6</sup> A. Yazdani, C. M. Howald, C. P. Lutz, A. Kapitulnik, and D. M. Eigler, Phys. Rev. Lett. **83**, 176 (1999).
- <sup>7</sup> S. H. Pan, E. W. Hudson, K. M. Lang, H. Eisaki, S. Uchida, and J. C. Davis, Nature **403**, 746 (2000).
- <sup>8</sup> J. X. Zhu and C. S. Ting, Phys. Rev. B **64**, 060501 (2001).
- <sup>9</sup> A. Polkovnikov, S. Sachdev, and M. Vojta, Phys. Rev. Lett. **86**, 296 (2000).
- <sup>10</sup> I. Martin, A. V. Balatsky, and J. Zaanen, Phys. Rev. Lett. **88**, 097003 (2002).
- <sup>11</sup> J. X. Zhu, C. S. Ting, and C. -R. Hu, Phys. Rev. B **62**, 6027 (2000).
- <sup>12</sup> N. Nagaosa and P. A. Lee, Phys. Rev. Lett. **79**, 3755 (1997).
- <sup>13</sup> J. X. Zhu and C. S. Ting, Phys. Rev. B **63**, 020506 (2000).
- <sup>14</sup> J. Bobroff, W. A. MacFarlane, H. Alloul, P. Mendels, N. Blanchard, G. Collin, and J. -F. Marucco, Phys. Rev. Lett. **83**, 4381 (1999).
- <sup>15</sup> M. -H. Julien, T. Fehér, M. Horvatić, C. Berthier, O. N. Bakharev, P. Ségransan, G. Collin, and J. -F. Marucco, Phys. Rev. Lett. **84**, 3422 (2000).
- <sup>16</sup> J. Bobroff, H. Alloul, W. A. MacFarlane, P. Mendels, N. Blanchard, G. Collin, and J. -F. Marucco, Phys. Rev. Lett. **86**, 4116 (2001).
- <sup>17</sup> H. F. Fong, P. Bourges, Y. Sidis, L. P. Regnault, J. Bossy, A. Ivanov, D. L. Millius, I. A. Aksay, B. Keimer, Phys. Rev. Lett. **82**, 1939 (1999).
- <sup>18</sup> Y. Sidis, P. Bourges, H. F. Fong, B. Keimer, L. P. Regnault, J. Bossy, A. Ivanov, B. Hennion, P. Gautier-Picard, G. Collin, D. L. Millius, I. A. Aksay, Phys. Rev. Lett. **84**, 5900 (2000).
- <sup>19</sup> M. U. Ubbens and P. A. Lee, Phys. Rev. B **46**, 8434 (1992).
- <sup>20</sup> S. E. Barnes, J. Phys. F **6**, 1375 (1976).
- <sup>21</sup> P. Coleman, Phys. Rev. B **29**, 3025 (1984).
- <sup>22</sup> G. M. Zhang, H. Hu, and L. Yu, Phys. Rev. Lett. **86**, 704 (2001).
- <sup>23</sup> Y. Wang and A. H. MacDonald, Phys. Rev. B **52**, R3876 (1995).
- <sup>24</sup> M. Takigawa, M. Ichioka, and K. Machida, Phys. Rev. Lett. **83**, 3057 (1999).
- <sup>25</sup> J. X. Zhu, and C. S. Ting, Phys. Rev. Lett. **87**, 147002 (2001).
- <sup>26</sup> Q. -H. Wang, J. H. Han, and D. -H. Lee, Phys. Rev. Lett. **87**, 167004 (2001).
- <sup>27</sup> Q. Han, Z. D. Wang, L. -Y. Zhang, and X. -G. Li, Phys. Rev. B **65**, 064527 (2002).
- <sup>28</sup> Q. Han, Z. D. Wang, and L. -Y. Zhang, Phys. Rev. B **62**, 5936 (2000).
- <sup>29</sup> J. X. Zhu, C. S. Ting, and A. V. Balatsky, cond-mat/0109503 (2001).
- <sup>30</sup> In Ref.<sup>29</sup>, a small energy gap is chosen and lead to single LDOS peak in the vortex center corresponding to the core states, which is comparable to the LDOS peak of a unitary impurity. Therefore, when a unitary impurity sits in the vortex center it is difficult to identify whether the impurity resonance is present in the vortex core or vortex core states are strengthened by the impurity.
- <sup>31</sup> K. V. Samokhin and M. B. Walker, Phys. Rev. B **64**, 024507 (2001).
- <sup>32</sup> M. Nielsen and P. Hedegård, Phys. Rev. B **51**, 7679 (1995).
- <sup>33</sup> N. -C. Yeh, C. -T. Chen, G. Hammerl, J. Mannhart, A. Schmehl, C. W. Schneider, R. R. Schulz, S. Tajima, K. Yoshida, D. Garrigus, and M. Strasik, Phys. Rev. Lett. **87**, 087003 (2001).

FIG. 1. LDOS versus energy at an NN site within the unitary impurity model for the cases (i) without vortex(dashed line), (ii) a vortex pinned at the impurity site (solid line), and (3) a vortex core without impurity (dotted line). The bulk density of states is also plotted for reference (dash-dotted line). Inset shows the spatial distribution of the LDOS at energy  $E_0/\Delta_{max} = -0.02$  in a  $16 \times 16$  region for case (i).

FIG. 2. LDOS versus energy at the impurity site (solid line), NNN site (dashed line), and NN site (dotted line) under zero field within the extended Anderson impurity model. The bulk density of states is also plotted for reference (dash-dotted line). Inset (a) shows the variation of  $\Delta F$  as a function of  $\lambda_0$  and (b) gives the spatial distribution of the LDOS at energy  $E_0/\Delta_{max} = -0.04$ .

FIG. 3. Same as Fig. 2 except that a vortex is pinned on the impurity site. Inset (b) gives the spatial distribution of the LDOS at energy  $E_0/\Delta_{max} = 0.02$ .

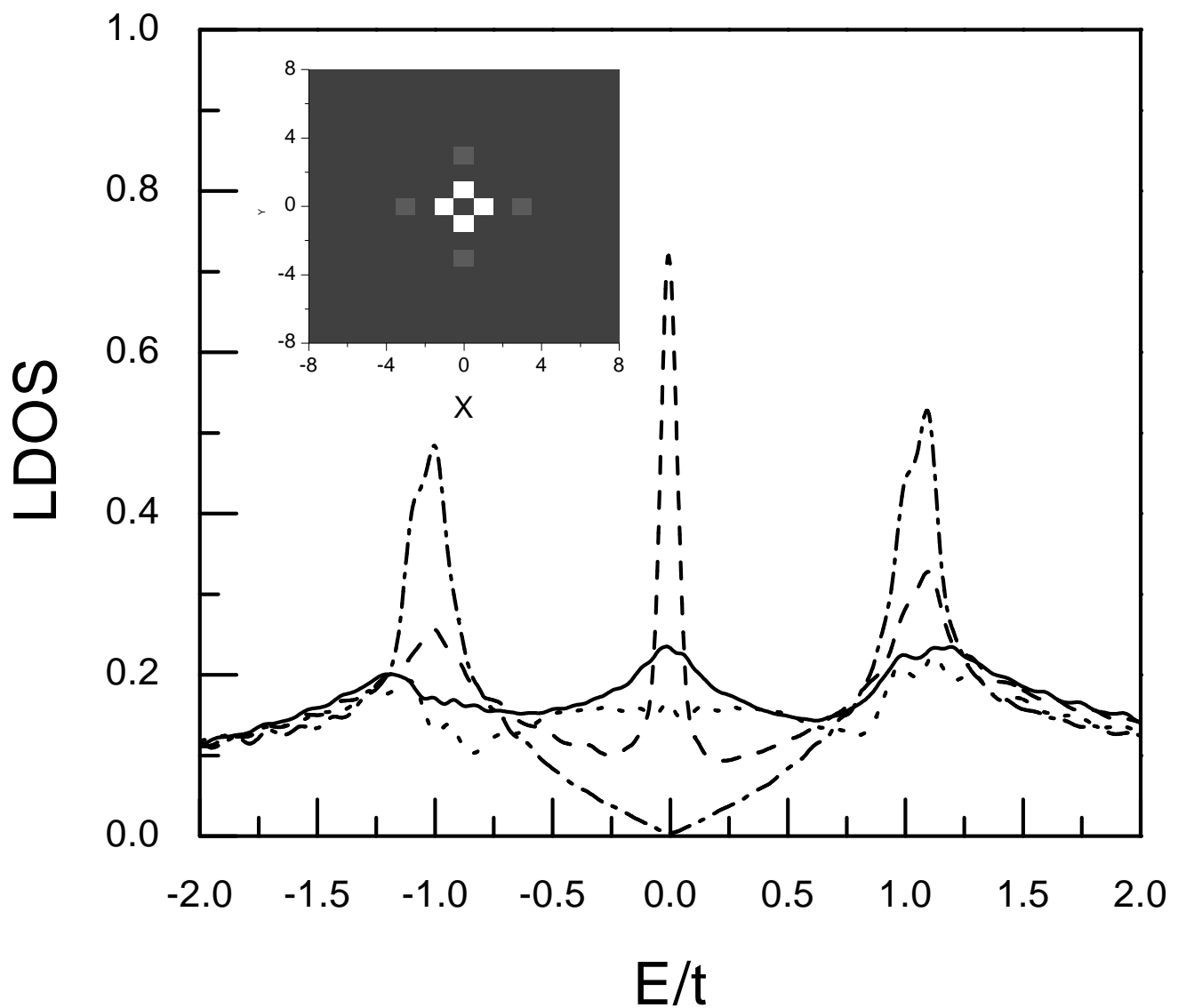


Fig. 1 Han et al

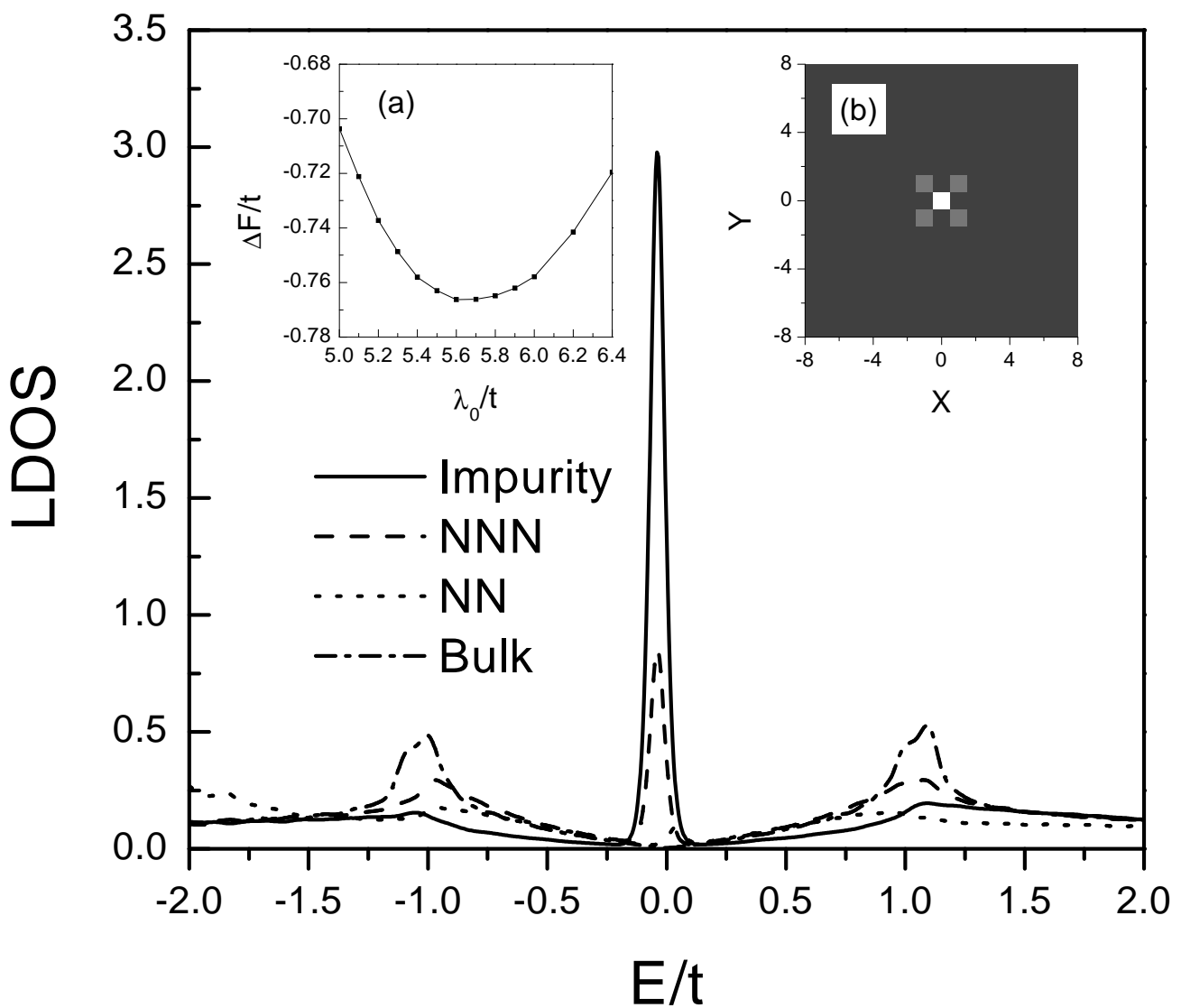


Fig. 2 Han et al

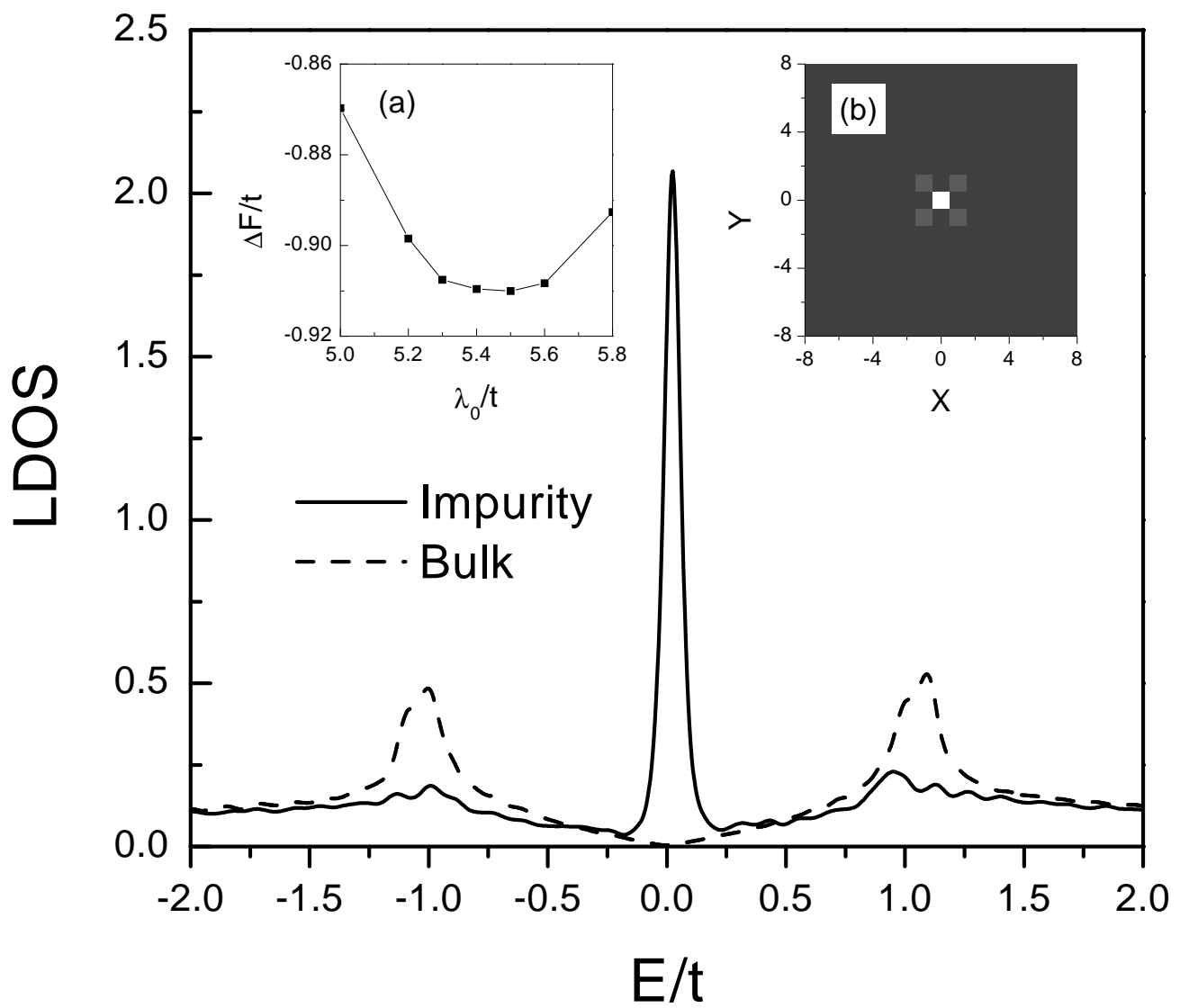


Fig. 3 Han et al